

# THE E.DEORBIT CDF STUDY: A DESIGN STUDY FOR THE SAFE REMOVAL OF A LARGE SPACE DEBRIS

Robin Biesbroek<sup>(1)</sup>, Tiago Soares<sup>(1)</sup>, Jakob Hüsing<sup>(1)</sup>, Luisa Innocenti<sup>(2)</sup>

<sup>(1)</sup> ESA/ESTEC, Keplerlaan 1, 2201AZ Noordwijk, The Netherlands, Email: robin.biesbroek@esa.int, tiago.soares@esa.int, Jakob.huesing@esa.int

<sup>(2)</sup> ESA/HQ Daumesnil, 52 rue Jacques Hillairet, 75012 Paris, France, Email: luisa.innocenti@esa.int

## ABSTRACT

In the period June to September 2012 the European Space Agency conducted a pre-assessment study in order to produce preliminary system designs for capturing a large space Debris, identify their required technology roadmaps, and investigate their applicability to other ESA missions. The study was carried out by an interdisciplinary team of specialists from ESTEC and ESOC within the Concurrent Design Facility (CDF), and was financed by the Clean Space branch 4 initiative.

The paper will highlight the details of the trade-off, the design of the sub-systems, the results of various capturing and rendezvous simulations, plus the assessment on cost, risk and programmatic. Finally, it gives a summary of the proposed roadmaps for this mission.

## 1 THE E.DEORBIT MISSION AND STUDY

The e.Deorbit mission is to perform active space debris removal of an uncooperative target (large satellite or upper stage) with heavy mass, of which its orbit resides in the 800 - 1000 km (near) polar region. Figure 1 gives the mission outline.

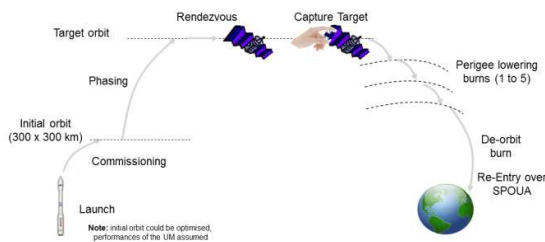


Figure 1. e.Deorbit mission outline

The mission shall be compatible with launcher from the European family (VEGA, Soyuz from Kourou, or Ariane), be launched by 2021, perform a safe rendezvous and mating with the target, de-orbit the target without creating extra debris that does not decay within 25 years, and ensure a safe controlled re-entry into the South Pacific Ocean Uninhabited Area (SPOUA) with a casualty risk below  $2 \cdot 10^{-5}$ . It should be noted though that the casualty risk is taken from

France's "Space Operations Act", whereas the ISO 24113, likely to be adopted by ESA in 2013, indicates a casualty risk of  $1 \cdot 10^{-4}$ .

A pre-assessment study was performed by a team from the CDF, a state-of-the-art facility equipped with a network of computers, multimedia devices and software tools, which allows a team of experts from several disciplines to apply the concurrent engineering method to the design of future space missions [1]. The team consisted of: a Study manager, Team leader, two System Engineers, a Debris expert, engineers for mechanical and electrical sub-systems, including GNC and robotics, engineers for cost, risk, safety and programmatics, representatives for Human spaceflight and Earth Observations, and finally representatives for space agencies CNES, ASI and DLR.

The main tasks that the CDF team had to carry out were to:

- Assess the feasibility of a mission for the controlled de-orbiting and re-entry of a large target in Sun Synchronous Orbit, using technologies already analysed in previous CDF studies performed at ESA
- Perform a System level conceptual design of the spacecraft with the participation of all discipline specialists
- Trade-off different mission scenarios
- Assess programmatics, risk and cost aspects of the various alternatives
- Consolidate the Technology road maps in line with the programmatic aspects of the mission
- Evaluate the applicability of the technologies to different categories of satellites and debris remediation mission

## 2 THE TARGET

The target debris was supposed to be of 8 tonne mass class, uncooperative with a (near) Sun Synchronous Orbit at altitude of roughly 800 km. It was assumed that the launcher adapter interface is not accessible as a solar panel could get stuck in such a position that it blocks access.

The long term stability of the debris is unknown and therefore four scenarios had to be taken into account:

the solar panels aligned with the velocity vector but the Y-axis is aligned either in velocity or anti-velocity direction. Then for both these cases the X-axis points either to nadir or zenith, making four cases in total. The target is not assumed to be fixed in attitude: the possibility of oscillation around the equilibrium with angular rates  $< 0.1 \text{ }^\circ/\text{s}$  is taken into account. In case it was necessary for the CDF team to use a target example, ESA's Envisat satellite was used, see Figure 2.

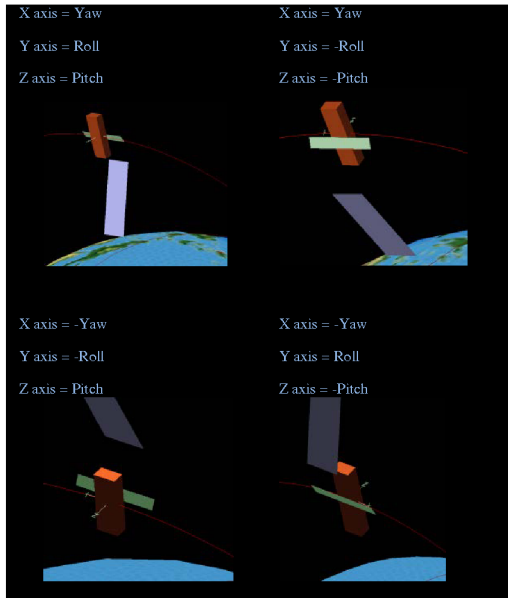


Figure 2. Possible long-term attitudes assumed for the target

Furthermore the risk of break-up and exploding of the target was assessed as it was assumed that the target won't be passivated. An analysis of fragmentation events in the DISCOS database was done where it was found that in total 257 events occurred. Out of those 257 events, 131 events were payload related (i.e. not rocket stage) and therefore relevant for the analysis. From those 131 events, 58 break-ups were deliberate, 4 were collision events, 11 events were aerodynamic related, which means that 58 events remain relevant for the analysis. Figure 3 shows the break-ups per mission type.

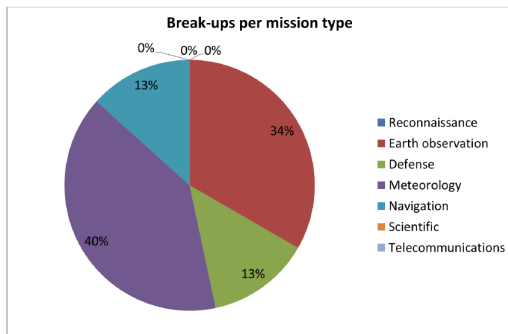


Figure 3. Break-ups per mission type.

The analysis concentrated on SSO missions only and excluded (Russian) Reconnaissance, which leaves only 15 events. This implies that the statistics give low confidence however from the relevant events the CDF team assumes that the target is still intact after 10 years in orbit.

Another issue to be taken into account is the risk of explosion, caused by a capturing manoeuvre: a risk present due to non-passivation of tanks, implying possible propellant residuals in tanks. Over a period of several years, propellant decomposition could occur, leading to corrosion of tanks. This, in turn, has an impact on the structural integrity of the tanks and might lead to risk of tank explosions.

The risk analysis concluded that tanks are usually thermally decoupled: consisting of low conductivity brackets, low emissivity blankets, and heaters.

A thermal analysis showed that in the long-term attitude, tank radiator exposure to direct sunlight over long time periods appear unlikely, which results in the propellant being frozen, and therefore leading to no corrosive environment.

Explosion could also be caused by tank puncturing, however all propellant tanks are located inside the central cylinder and are therefore well protected from e.g. clamping mechanisms. For penetrating devices such as harpoons, the harpoon target point should be selected carefully though not to puncture a tank.

Finally, the risk of thruster break-off and propellant leaking due to manipulation, was assessed. This could be caused by entanglement in a net, hitting / bending by clamping mechanisms, for example. In these cases it is likely that only the nozzle breaks off. The valve is located upstream of the nozzle and upstream of the flange with which the thruster is mounted to the spacecraft. This means that it is likely that the valve remains intact and closed, in which case leaking does not occur.

From a legal point of view, the Outer Space Treaty and Liability Convention, as recorded in UNCOPUOS (United Nations Committee on Peaceful Uses of Outer Space) state that the launching state has jurisdiction over the launched object, and remains liable even when it stopped functioning (note that ESA is a launching state). This means that if the target is not launched by ESA, approval is needed from the target registration state. For this reason, the CDF team assumed the target to be ESA owned. Even so, if the member states participating in the chaser satellite development are different from the member states of the target satellite, approval from the target member states that are not chaser members states is needed.

### 3 SYSTEM OPTIONS AND TRADE-OFF

Several options were assessed in terms of disposal orbits (re-orbit to over 2000 km altitude, de-orbit to below 600 km altitude, and de-orbit into the atmosphere using a controlled re-entry), propulsion options (electrical, chemical or a combination), and capture techniques (pushing techniques such as robotic arm and clamping mechanisms, pulling techniques such as a net or harpoon, and touch-less techniques such as an ion-beam shepherd).

In terms of orbit options, the ‘de-orbiting to an altitude below 600 km’ does not comply with the casualty risk required for this mission, as the target mass is so large (+ 8000 kg) that the casualty risk when doing an uncontrolled re-entry within 25 years is higher than  $2 \cdot 10^{-5}$ . For the re-orbit case it is not possible to calculate the casualty risk. Re-orbiting does not prevent an uncontrolled de-orbit but the re-entry is postponed by hundreds of thousands of years. Not knowing the population growth on Earth in hundreds of thousands of years, it is not possible to prove the casualty risk. In fact, in the likely case that human population keeps growing, the casualty risk also grows. Furthermore from a propulsion point of view, the propellant required to re-orbit is larger than the propellant required to perform a controlled re-entry, when using a chemical propulsion system. A more viable case to re-orbit would be the use of electrical propulsion as it combines low forces acting on the target, with low propellant consumption on the chaser. However with the related cost impact, implementation of a capturing mechanism and GNC control development, the cost of such a system is of the same order as the cost of a chemical propulsion based system that performs a controlled re-entry. It is for these reasons that a controlled re-entry was the preferred option.

Capturing techniques considered during this study are extensively described in [2]. During the study it was decided to focus on both a pushing technique and a pulling technique, to assess the impacts on the spacecraft design. From the pushing techniques, robotic arms and clamping mechanisms were considered. From pulling techniques, a capture using a net was considered. These capture techniques were considered most applicable to wide variety of target shapes, while minimizing the probability of creating extra debris. Figure 4 shows the trade-off tables with various criteria considered. Colour codes are used to indicate good (green), average (yellow) or not good (red). From the options considered, options 3a and 3b were selected for further study, as they combined green highlights for cost, time to re-enter, and several risks such as the casualty risk.

Option	Short description	Cost	Time to re-entry (yr)	Technical risk	Risk of casualties	Risk of extra debris	Risk of mission terminating impacts	Risk of target catastrophic collision accumulated from 2012 to decay	Programmatic risk	Comments
1 a)	All CP, net, re-orbit to 2000 km	Yellow	Infinite	Critical 3C	Unknown	Major 2B	$4.529 \cdot 10^4$	$0.016$ in 2200, no decay	Critical 3C	Result in two debris objects in 2020 km
1 b)	EP/CP, robotic arm, re-orbit to 2000 km	Yellow	Infinite	Major 3A	Unknown	Critical 2C	$4.529 \cdot 10^4$	$0.016$ in 2200, no decay	Major 3A	Result in two debris objects in 2020 km

Option	Short description	Cost	Time to re-entry (yr)	Technical risk	Risk of casualties	Risk of extra debris	Risk of mission terminating impacts	Risk of target catastrophic collision accumulated from 2012 to decay	Programmatic risk	Comments
2 a)	All EP, ion-beam, de-orbit to 600 km	Green	36	Critical 3B	$> 5 \times 10^{-3}$	Significant 2A	$3.429 \cdot 10^4$	0.052	Critical 3C	Immature concept
2 b)	All EP, net, de-orbit to 600 km	Green	36	Critical 3C	$> 5 \times 10^{-3}$	Major 2B	$1.381 \cdot 10^4$	0.052	Critical 3C	AOCG with no debris
2 c)	EP/CP, robotic arm, de-orbit to 600 km	Green	36	Major 3A	$> 5 \times 10^{-3}$	Critical 2C	$1.381 \cdot 10^4$	0.052	Major 3A	CP needed for softing
2 d)	EP/CP, tentacles, de-orbit to 600 km	Green	36	Critical 3B	$> 5 \times 10^{-3}$	Major 2B	$1.381 \cdot 10^4$	0.052	Critical 3B	CP needed for softing
2 e)	All CP, tentacles, de-orbit to 600 km	Green	35	Critical 3B	$> 5 \times 10^{-3}$	Major 2B	$1.877 \cdot 10^4$	0.052	Critical 3B	cheapest option

Option	Short description	Cost	Time to re-entry (yr)	Technical risk	Risk of casualties	Risk of extra debris	Risk of mission terminating impacts	Risk of target catastrophic collision accumulated from 2012 to decay	Programmatic risk	Comments
3 a)	All CP, net, controlled re-entry	Green	10	Critical 3C	$< 10^{-6}$	Major 2B	$1.877 \cdot 10^4$	0.0075	Critical 3C	Low cost & dark TRC/VEGA
3 b)	All CP, tentacles, controlled re-entry	Green	10	Critical 3B	$< 10^{-6}$	Major 2B	$1.877 \cdot 10^4$	0.0075	Critical 3B	Low cost & dark TRC/VEGA
3 c)	All CP, robotic arm + clamping, controlled re-entry	Yellow	10	Critical 3B	$< 10^{-6}$	Critical 2C	$1.877 \cdot 10^4$	0.0075	Critical 3B	Low cost & dark TRC/VEGA
3 d)	EP/CP, net controlled re-entry	Yellow	11	Critical 3C	$< 10^{-6}$	Major 2B	$2.252 \cdot 10^4$	0.0075	Critical 3C	Two propulsion systems
3 e)	EP/CP, tentacles, controlled re-entry	Yellow	11	Critical 3B	$< 10^{-6}$	Major 2B	$2.252 \cdot 10^4$	0.0075	Critical 3B	Two propulsion systems
3 f)	EP/CP, robotic arm + clamping, controlled re-entry	Yellow	11	Critical 3B	$< 10^{-6}$	Critical 2C	$2.252 \cdot 10^4$	0.0075	Critical 3B	Complex design, 2x propulsion, 2x grasping
VAC1)	All CP, tentacles, controlled re-entry	Yellow	10	Critical 3B	$< 10^{-6}$	Major 2B	$1.877 \cdot 10^4$	0.0075	Critical 3B	Reuse ESA net main data/eharad
VAC2)	All CP, robotic arm + clamping, controlled re-entry	Yellow	10	Critical 3C	$< 10^{-6}$	Critical 2C	$1.877 \cdot 10^4$	0.0075	Critical 3B	Reuse ESA net main data/eharad

Figure 4. Systems trade-off table

Option 3a indicates a platform based on chemical propulsion, using a net to capture the target, and performing a controlled re-entry.

Option 3b indicates a platform based on chemical propulsion, using clamping mechanisms to capture the target, and also performing a controlled re-entry.

Both options are discussed in the next two sections.

### 4 THE NET OPTION

The net option system design is based on a VEGA launch, and therefore uses a 937 mm central cylinder to match the VEGA interface adapter. Also the total wet mass is 1622 kg including the launcher adapter interface, that corresponds to the VEGA performance into a 300 km circular orbit at  $98.2^\circ$  inclination.

After launch, several launcher dispersion correction manoeuvres are performed, for which a total  $\Delta V$  of 7 m/s is allocated. The spacecraft will then raise its orbit to obtain an altitude of 5 km below the altitude of the target spacecraft ( $\Delta V$  allocated: 260 m/s). The orbit raising may be performed in several phases in order to minimise gravity losses. The small difference in final altitude allows the chaser to drift towards the target.

For the rendezvous, an approach similar to ESA’s ATV mission is proposed where the final altitude of the chaser and target is met, followed by several hops along the V-bar to approach the target, see Figure 5.

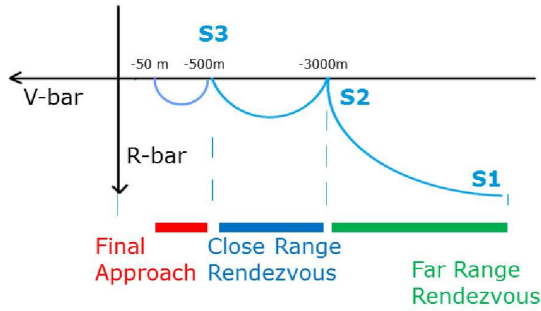


Figure 5. RDV overview for the net option

After reaching point S3, radial hops and a forced motion is used to reach a distance of roughly 50 m. At this distance, ground observation of the target is performed, as well as characterisation of the target's rotation. Then, from a distance currently assumed at 20m, the net is deployed towards the target. In case a Collision Avoidance Manoeuvre (CAM) is required, the spacecraft could simply manoeuvre back to point S2. Even if loss of control occurs, due to the nature of the approach the chaser will not hit the target during the first orbit.

250 multi-body simulations of the net capture have been performed during the CDF study, each with 6000 degrees of freedom. A net mesh of 2 m was used in order to save computation time, however the proposal is to use a mesh of 25 cm. The following parameters were systematically varied to check the sensitivity to these parameters: Relative position up to 2 m (3 axis), relative rotation up to 5° (3 angles), relative rotation rates up to 3°/sec (3 axis), relative motion up to 10 cm/s (3 axis), tether length, tether stiffness, tether material damping and control strategy. None of the variations in the position and rotation parameters had a noticeable effect. Only in 2% of all cases, detachment or partial detachment occurred, and only for simulated cases with high rotation rate around the local horizontal. The risk of detachment can easily be mitigated by inserting net closure mechanisms. Figure 6 shows an animated sequence of the net deployment.

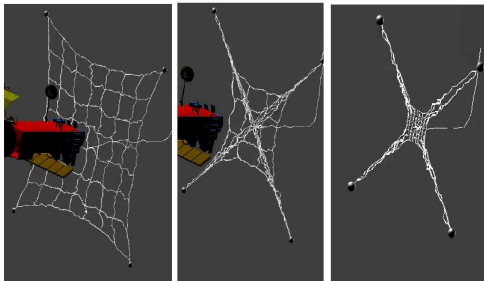


Figure 6. Net deployment

After capture, the chaser actuators must stabilise the

chaser attitude, orient to Sun until the time of starting the de-orbiting sequence, and finally orient to the burn direction.

The net simulations also included the de-orbit burns. In order to minimise the sum of thrusters and the propellant required for de-orbiting, a sequence of 3 + 1 manoeuvres is proposed. This implies lowering the perigee to an altitude of about 200 km using three burns, followed by a final burn for the re-entry, see Figure 7.

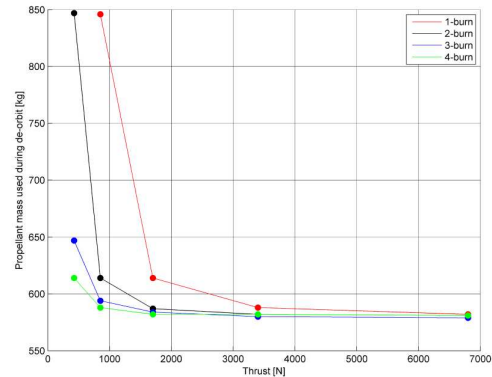


Figure 7. Propellant due to gravity losses for the net option

A simple control algorithm was implemented in the simulator to control both position (keep target and chaser aligned on orbital track) and attitude (of the chaser), while investigating different tether length, stiffness and material damping. In terms of control requirements, the tested controllers had no problem tensioning the system after capture. No significant rotational velocity or pendulum motion occurred. However the tested controllers did have problems recovering smoothly at the end of the burn, although eventually position control was re-established. A number of strategies are possible for mitigating this immediate re-entry: using 1 burn (which requires thrusters and therefore more mass, see Figure 7), throttleable engines, or adding 220N pulse mode engines. The latter option was chosen as baseline. There was a overshoot period at the end of the burn in which the tether went slack. The controller was unable to avoid this.

In principle most dynamic problems are reduced by increasing tether length: it leads to smaller torque requirements on chaser (generally around 2 Nm for a 420 meter tether), there is no risk of collision, and leads to lower stiffness (slower oscillations which lead to lower bandwidth requirements for controller). However a longer tether requires more time (and propellant) for the tensioning phase. A 400 m tether is therefore proposed.

A stiffer tether reduces amplitude of oscillations in the

distance between the spacecraft. The maximum allowed tether stiffness is driven principally by the controller bandwidth: the maximum possible stiffness from this point of view should be significantly higher than the  $k=47$  value simulated. It should be noted that the overshoot can be avoided entirely even if the oscillations are not damped. This can be achieved by ending the de-orbit burn when tether tension is at its minimum (and relative velocity is zero), as is shown in Figure 8.

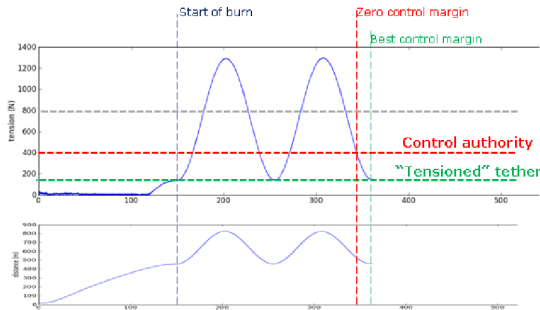


Figure 8. Illustration of the control margin available as a function of the phase of the oscillations when the burn ends. The top plot is the tension in the tether, and the bottom plot is the distance between the spacecraft

When firing the thrusters for the de-orbit burns, the thrust plumes are directed towards the deployed tether, as it is a pulling technique. Figure 9 shows the heat fluxes acting on the tether. Several configurations for the thrusters have been tested. When using four thrusters (which in turn could limit the amount of de-orbit burns to only one), the heat flux on the tether is  $3 \text{ MW/m}^2$  within the first two meters from the chaser. To overcome this problem, three strategies were tested: limiting to only two thrusters, tilting the thrusters, or placing the thrusters on the side walls of the satellite, therefore shielding the tether using the side walls. When using two thrusters, the temperature of the tether still leads to  $1000 - 1200\text{K}$  within the first three meters, requiring that part to be replaced by for example steel. Tilting the thrusters leads to high losses in manoeuvre efficiency, raising the wet mass of the satellite above the VEGA performance. Placing the thrusters on the side of the satellite puts a heat flux of  $0.5 \text{ MW/m}^2$  on to the side walls, requiring therefore a Thermal Protection System (TPS) to be placed on the walls. Furthermore this option poses problems fitting inside the VEGA fairing. Option one (two thrusters) was therefore chosen as baseline. Zylon could be considered as tether material (density  $1550\text{kg/m}^3$ , heat capacity  $2000 \text{ J/kg/K}$ ).

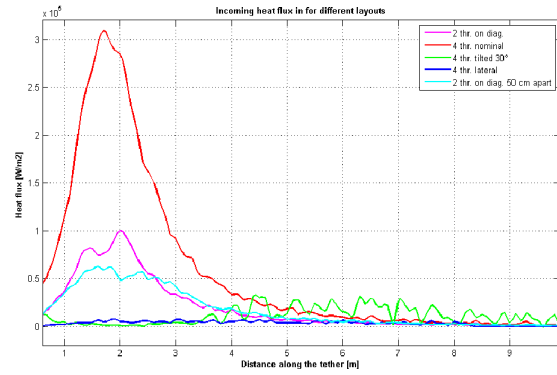


Figure 9. Incoming heat flux on tether for different thruster layouts

The SPOUA dimensions are  $7000 \text{ km}$  in longitudinal direction, and  $3000 \text{ km}$  in latitudinal direction. Since the target orbit is assumed near-polar, the re-entry must therefore reduce the debris footprint to maximum  $3000 \text{ km}$ . An analysis of the debris footprint size (see Figure 10) showed that the final de-orbit burn must reduce the perigee altitude to  $40 \text{ km}$  or less, when an apogee of  $800 \text{ km}$  is used and break-up occurs at  $90 \text{ km}$  altitude. Thermal failure of the zylon tether is predicted at  $74 \text{ km}$ .

In case the propulsion system fails to fire the de-orbit burn, a new attempt can be made in the next day. An advantage of the multiple-burn strategy is that the system is ready for this: the  $220\text{N}$  thrusters will maintain the relative motion of the two spacecraft, even if the burn is cut off too soon. An option based on only one de-orbit burn will need a different contingency scheme if the de-orbit burns partially fails. Apart from the heat flux and mass minimisation, this is the third reason why a multiple-burn strategy was chosen.

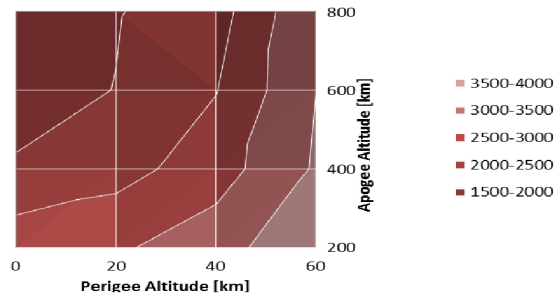


Figure 10. Footprint size as function of perigee and apogee altitudes

The chaser platform is shown in Figure 11 and is a box-shaped configuration with two deployable solar panels. The capture mechanism consists of two canisters containing the net plus tether, located on the top deck in between the thrusters. The attitude and orbit control (AOCS) subsystem contains star trackers, Sun sensors,

gyro meters, GPS receivers, LIDAR, and a far field camera. For the control, 22N thrusters are used. A bi-propellant propulsion system is installed using two (plus two redundant) 425N thrusters, as well as four 220N thrusters to be used in pulse mode. Four polar mounted tanks contain the propellant, plus three tanks for the pressuriser. An option not investigated in detail was to mount the net canisters on a long cylinder, allowing to mount eight thrusters (four active). This could reduce the number of de-orbit burns but leads to high TPS mass.

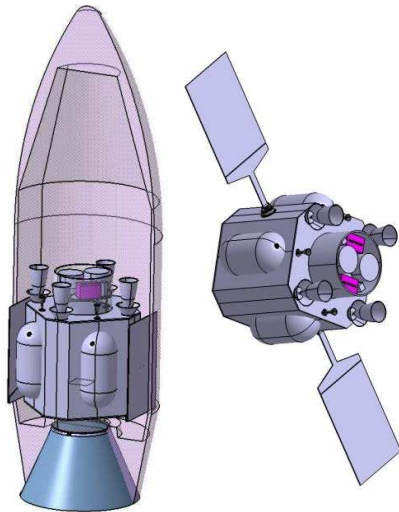


Figure 11. Clamping mechanisms option system design shown in stowed configuration (left) and de ployed configuration (right)

Two deployable triple-junction solar panels, with a total area of 2.8 m<sup>2</sup>, provide for 785 W of power at end of life. For the eclipses, a lithium-ion battery is used. All are based on a 28V multi-power-point-tracking unregulated bus.

In order to provide coverage of the entire rendezvous and capture process, a data relay with the TDRSS constellation is proposed. For this reason, a TDRS S-band antenna, transponder and diplexer, and high power amplifier are selected. For the direct-to-Earth communications, an X-band transponder and omni-antenna are selected. Data handling is done using a dynamically configurable payload processor (DRPM). The thermal sub-system is standard using multi-layer insulation, optical Sun reflectors, black paint, heaters and heat pipes.

Apart from solar array deployment and drive mechanisms, the tether and net are deployed using a net ejector. Two tether canisters are baselined for redundancy. This requires the presence of a tether cutter in case the contingency net is to be used.

The development schedule predicts a launch date in August 2021, taking into account a contingency of 10%.

The dry mass of the system is 709 kg, excluding launcher adapter. Total propellant mass is 878 kg.

## 5 THE CLAMPING MECHNISMS OPTION

The clamping mechanism option system design is also based on a VEGA launch, but in contrast to the net option has a rectangular shape with a central shear panel and stiffeners for the tank panels. The total wet mass is 1648 kg including the launcher adapter interface, which also matches the 1660 kg VEGA performance into a 300 km circular orbit at 98.2° inclination. Similar to the net option, the launch is followed by launcher dispersion correction manoeuvres and manoeuvres to raise the orbit to be 5 km below the target altitude.

For the rendezvous, the final approach to a distance of 50 m is similar to the net option as shown in Figure 5, however from 50 m on the sequence is different as the chaser needs to approach to 0 m of the target. For this reason, a matching of the target's rotation using a forced motion while approaching to 1 m is required, shown in Figure 12. From 1 m on, the GNC system is switched off and the chaser will drift towards the target, while the tentacles close in to capture it. CAM sequence is the same as described in the net option.

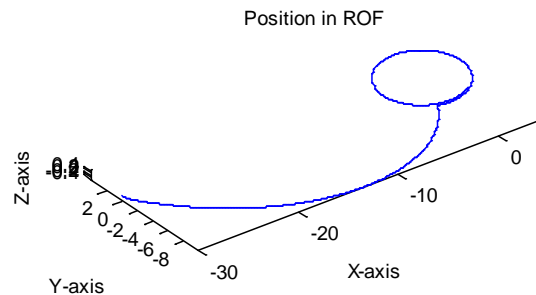


Figure 12. Rotation match by using forced motion

The strategy of the clamping mechanism is to embrace the target with 'tentacles' (i.e. arm-shaped clamping mechanisms) so that it cannot escape, and then to positively lock the tentacles with a force higher than the de-orbiting force. This requires using pushing rods based on an IBDM (International Berthing and Docking Mechanism) actuator. The composite (chaser + target) is then stiff during de-orbit operation. This method is generic : it can also be applied to the interface cone launcher, should this interface be accessible.

Several simulations of the clamping mechanism closing were performed, investigating the relative position change between target and chaser during the grabbing. As initial conditions, rotation errors of 0.05°/s in all axes were used, position errors of 1 mm in all axes,

rotation rate errors of 0.1°/s in all axes, and velocity errors of 2 mm/s in all axes. The allowable envelope was set by the GNC system to  $\pm 87$  mm in X-axis. A 20% margin was subtracted, giving 69 mm of maximum envelope. Simulation indicated a maximum relative position change of 61 mm as shown in Figure 13. This is therefore within the envelope but requires further testing when a more detailed design is available. It was seen that in some simulations, bouncing occurred.

The maximum relative position was kept within the envelope by using the following initial conditions: the tentacles were opened to maximum  $30^\circ$ , and the pushing rods were partially deployed 200 mm before the target. Furthermore the tentacles closing speed was set to  $5^\circ/\text{s}$  and the pushing rods deployment speed was set to 25 mm/s.

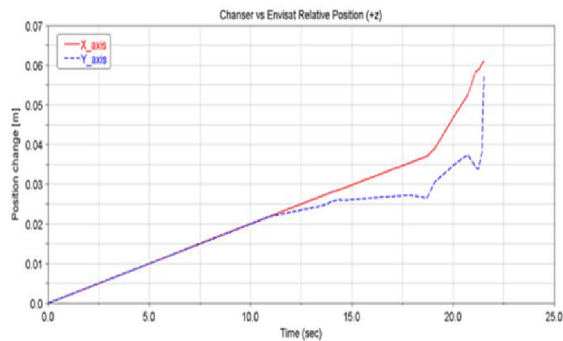


Figure 13. Relative positions when using clamping mechanism grabbing

One way to mitigate the risk of breaching the relative distance envelope is the use of a robotic arm, at the expense of an increase in cost. A first grabbing at the launcher adapter interface, using the robotic arm, could be performed. After establishing the connection, the robotic arm could guide the chaser to the exact position required, after which the clamping mechanisms and pushing rods will establish a firm fixation, see Figure 14.

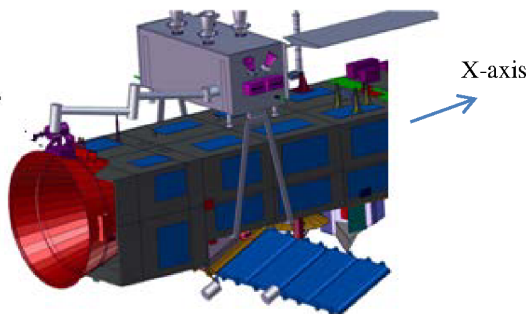


Figure 14. Example of using both robotic arm and clamping mechanism

Similar to the net option, a sequence of 3 + 1

manoeuvres is proposed in order to minimise gravity losses during the de-orbit burns.

A pushing technique is inherently more stringent on centre of gravity (CoG) alignment than a pulling technique. In particular for an 8000 kg class target, the disturbing momentum build-up is so high that it needs to be compensated immediately. If the capture mechanism (clamping mechanism and/or robotic arm) is not able to align servicer within 2 cm of combined CoG, then controllability is not ensured. If de-orbit thrust is even higher than  $2 \times 425\text{N}$ , then the margin shrinks further; this was a second reason to limit the thrusters to  $2 \times 425\text{N}$ , therefore requiring several de-orbit burns. The maximum misalignment with respect to the CoG of an 8000 kg class target that could physically be compensated by 10N thrusters is 6 cm, both longitudinal and lateral (see Figure 15). For this reason, AOCS thrusters were upgraded to 22 N.

What needs to be taken into account as well is that compensation with AOCS thrusters leads to increased fuel consumption. One way to mitigate this risk is the use of thruster orientation mechanisms. These exist for electrical propulsion thrusters but would be a new development for 425N thrusters.

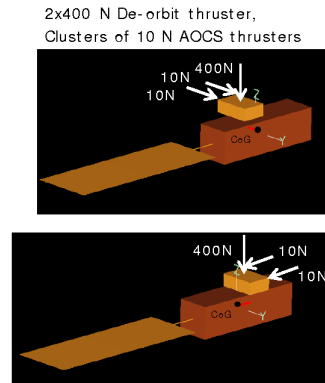


Figure 15. Illustration of the CoG misalignment compensation using 10N thrusters

De-orbiting sequence using the clamping mechanisms option is similar to the net option and described in the previous section.

The chaser platform is shown in Figure 16 and is a rectangular box-shaped configuration with one deployable solar panels. The capture mechanism consists of two clamping mechanisms stowed on the long side of the spacecraft. Note that the height of the spacecraft is determined by the size of the target spacecraft, as the chaser body needs to be wide enough to embrace the target spacecraft. For this reason, the configuration is launched side-ways. As the thrusters need to be on the opposite side of the clamping mechanisms, the propulsion system is launched side-

ways as well, which should be further investigated in a later phase. The attitude and orbit control subsystem contains star trackers, Sun sensors, Inertial Measurement Unit, GPS receivers, LIDAR, a far field camera, but in contrast to the net option also a near-field camera. For the control, 22N thrusters are used. A bi-propellant propulsion system is installed using two (plus two redundant) 425N thrusters. Four polar mounted tanks contain the propellant, plus two tanks for the pressuriser.



Figure 16. Clamping mechanisms option system design shown in stowed configuration (left) and de ployed configuration (right). This configuration shows the optional robotic arm on the right panel in the stowed configuration

One deployable triple-junction solar panels with an area of 2.8 m<sup>2</sup>, provides for 785 W of power at end of life. Similar to the net option, a lithium-ion battery is used for eclipses, while all are based on a 28B multi-power-point-tracking unregulated bus.

Thermal, communications and data handling sub-systems are all similar to the net option.

The mechanisms consist of the clamping mechanisms, including drive mechanisms, pushing rods, plus solar array deployment and drive mechanisms. An optional robotic arm is included in the design.

The development schedule predicts a launch date in February 2022, taking into account a contingency of 10%. This therefore just misses the requirement for a launch in 2021.

The dry mass of the system is 784 kg, excluding launcher adapter. Total propellant mass is 810 kg.

## 6 NEXT STEPS

Following the Ministerial Council of 2012, Clean Space

has initiated, or is initiating, several activities according to the Clean Space branch 4 roadmap [3].

Three system activities have started by the time of this conference, called ‘Service Oriented Approach towards the Procurement/Development of an ADR Mission’ where three consortia are studying how removal of a large ESA debris could be implemented as a service to ESA. Furthermore, the following activities in support of ADR capturing are planned to kick-off within the next half year: ‘Advanced GNC for ADR’ (net/tether control during burns), ‘Assessment And Simulation Of A tentacles Based Capture Mechanism for ADR’, and ‘Net Parametric Characterisation And Parabolic Test’. Other activities requested are: GNC activities (nav-cam, LIDAR, image recognition), net activities (winch, throwing mechanism), clamping mechanism activities (breadboard) and other sub-systems (Harpoon, reconfigurable payload processor).

The e.Deorbit Phase A is planned to kick-off after summer 2013.

## 7 REFERENCES

1. CDF home page. [www.esa.int/cdf](http://www.esa.int/cdf)
2. Wormnes, K., R. Le Letty, L. Summerer, H. Krag, R. Schonenborg, O. Dubois-Matra, E. Luraschi, and J. Delaval, K. Wormnes, R. Le Letty, L. Summerer, H. Krag, R. Schonenborg, O. Dubois-Matra, E. Luraschi, and J. Delaval, ‘ESA Technologies For Space Debris Remediation’, 6<sup>th</sup> European Conference on Space Debris, 6b.O-2, ID: 2818109, ESOC, 26 April 2013.
3. Innocenti, L., ‘ESA Clean Space Initiative’, 6<sup>th</sup> European Conference on Space Debris, 0.O-3, ID: 2818793, ESOC, 26 April 2013..